Journal of ELECTRONIC MATERIALS
https://doi.org/10.1007/s11664-019-07630-8

Growth, Optical, Thermal, Mechanical, Laser Damage Threshold and Electrical Polarizability of Cadmium Chloride Doped L-Alanine (LACC) Single Crystal for Optoelectronic Applications

C. KARNAN ,[1,4] A.R. PRABAKARAN,[1] M. PRABHAHARAN,[2] and G. VINITHA[3]

1.—Department of Physics, Pachaiyappa's College, University of Madras, Chennai 600 030, India. 2.—Department of Physics, Annai Violet Arts and Science College, University of Madras, Chennai 600 053, India. 3.—Division of Physics, School of Advanced Sciences, VIT University, Chennai 600127, India. 4.—e-mail: c.karnan@yahoo.com

L-Alanine doped with cadmium chloride crystal was grown by slow evaporation technique in an optimum condition using de-ionized water as solvent. Single crystal x-ray diffraction analysis was carried out to confirm the unit cell parameters and cell volume. The presence of amine vibrations and carboxylic acid vibrations affirm the presence of L-alanine in grown material by Fourier transform infrared (FT-IR) analysis. The ultraviolet visible near-infrared region (UV–Vis-NIR) spectrum revealed that the grown crystal has a lower cut-off wavelength at 246 nm and has high transmission in the entire visible region. Further, energy gap and the refractive index of the crystal were also calculated. Thermo-gravimetric (TG) and differential thermal analysis (DTA) were carried out, and it is estimated that the material is thermally stable up to 233°C and the melting point of the crystal was found to be 298°C. The mechanical strength of the material is estimated for various loads using Vicker's microhardness and it reveals that material belongs to a soft material category. The electrical polarizability was calculated using known values such as valence electron, molecular weight, energy gap and density of the material. Z-scan technique for nonlinear studies was carried out on a LACC crystal to determine the third order nonlinear absorption (β), nonlinear refractive index (n_2) and third order nonlinear susceptibility ($\chi^{(3)}$) using continuous wave Nd: YAG laser of 532 nm. Grown crystal shows that the material is very much suitable for second harmonic generation for frequency conversion applications.

Key words: X-ray diffraction, FT-IR, microhardness, TG-DTA, electrical polarizability, LDT, Z-scan technique

INTRODUCTION

In recent years, crystals possessing nonlinear optical properties were given more attention due to their applications in photonics, optoelectronics, frequency doubling, device fabrication, laser-based imaging, parametric amplifier, image reconstruction and data storage.[1–4] The renewed interest to study amino acid single crystals is because of their high second harmonic efficiency mainly attributed to the presence of π bonds.[5] Moreover, amino acids are bipolar in nature due to the presence of a deprotonated carboxylic group (COO^-) and a protonated amine group ($-NH_3^+$) known as Zwitterions.[6–8] The carboxyl group present in amino acids has potential ability to increase the charge mobility

(Received December 27, 2018; accepted September 6, 2019)

Published online: 17 September 2019

and photochemical stability of a crystal. All the compounds in this class contain optically active carbon atoms and thereby forming acentric crystals. Among the amino acids, L-alanine is an efficient nonlinear optical material because of its chirality which induces an asymmetric molecular structure.[9] In this regard, incorporating a suitable dopant over amino acid materials enhances many important properties.[10] The thermal stability of L-alanine is relatively higher than other amino acids.[11] According to the literature, cadmium chloride is a suitable dopant which enhances the thermal and mechanical stability of the organic crystal. In the present work, cadmium chloride doped L-alanine (LACC) crystals were grown from aqueous solution by slow evaporation method. Then 0.1 mol of cadmium chloride was doped in 1 mol of L-alanine. Grown crystals were subjected to instrumental analysis for characterization by x-ray diffraction, UV–Vis-NIR thermal, mechanical, electronic polarizability, second harmonic generation efficiency and third order nonlinear optical properties.

EXPERIMENTAL DETAILS

Synthesis and Growth

Cadmium chloride doped L-alanine single crystals were synthesized using L-alanine (LOBA) and cadmium chloride (MERCK) in a 1:0.1 molar ratio. Deionized water was used as a solvent. The solution was stirred continuously for 4 h using a magnetic stirrer to attain homogeneity. The obtained saturated solution was filtered using Whatman filter paper and covered with a perforated paper for slow evaporation in a dust free environment. After a week, good quality seed crystals were harvested. The harvested seed was immersed in mother solution. Good quality crystals were harvested after 37 days. Figure 1 shows the as grown crystal of Cadmium Chloride doped L-alanine crystal.

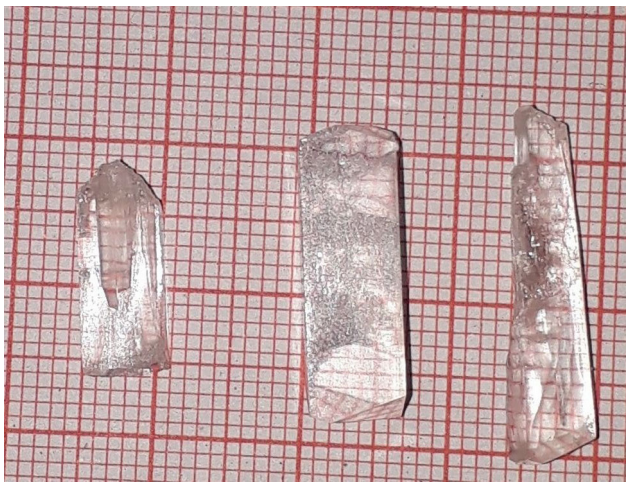

Fig. 1. As-grown LACC crystal.

Characterization Method

Cadmium Chloride doped L-alanine crystals were characterized using various techniques like single crystal x-ray diffraction, powder x-ray diffraction, Fourier Transform Infrared (FTIR), UV–Vis-NIR spectral, TG-DSC, electronic polarizability and nonlinear optical (NLO) studies. Single crystal x-ray diffraction was performed using BRUKER APEX 2 with MoKα (λ = 0.71073 Å) radiation. The powder x-ray diffraction was performed using BRUKER APEX 2 CuKα (λ = 1.5406 Å) with step size 0.034 s to measure the strain value. The FTIR spectrum was recorded by KBr pellet technique between the range 4000–400 cm^{-1}. The UV–Vis-NIR transmission was carried out using Perkin Elmer LAMDA 950 in the range 200–900 nm. TG-DTA was performed using NETZSCH STA 449 F3 Jupiter thermal analyser to measure the thermal stability of the crystals. The microhardness analysis was carried out using a Shimadzu microhardness analyzer. The second harmonic generation was detected using Kurtz Perry powder technique. Z-scan was carried out using a 532 nm diode pumped Nd: YAG laser source.

RESULTS AND DISCUSSION

XRD Analysis

Single Crystal XRD

Single crystal x-ray diffraction studies were carried using BRUKER APEX 2 with MoKα (λ = 0.71073 Å) radiation. The x-ray diffraction analysis affirms that the LACC crystal belongs to orthorhombic crystal system, and the unit cell parameters are a = 5.83 Å, b = 6.08 Å and c = 12.44 Å, $\alpha = \beta = \gamma = 90°$, and the cell volume V = 441 $Å^3$. The cell parameter values of LACC crystal agrees with the earlier reported values of pure L-alanine.[5,11–13]

Powder XRD

The powder diffraction studies were carried out using BRUKER APEX 2 CuKα (λ = 1.5406 Å) at the optimum condition and the pattern was recorded over a range of 10°C to 70°C with step size 0.034 s. Figure 2 shows the powder x-ray diffraction pattern of LACC crystal. The crystallinity nature of the crystal is confirmed by the sharp peaks and the peaks were indexed. The strain (η) present in the grown crystal was calculated using the Hall–Williamson relation.[14,15]

$$\beta \cos\theta = \frac{k\lambda}{\tau} + \eta \sin\theta, \qquad (1)$$

where β is full width at half maxima, θ is the angle of diffraction, k is Scherrer constant, λ is wavelength of x-rays, τ is crystallite size and η is a strain. Figure 3 shows the plot between $\beta\cos\theta$ versus $\sin\theta$. The strain value, η found from the slope of the graph

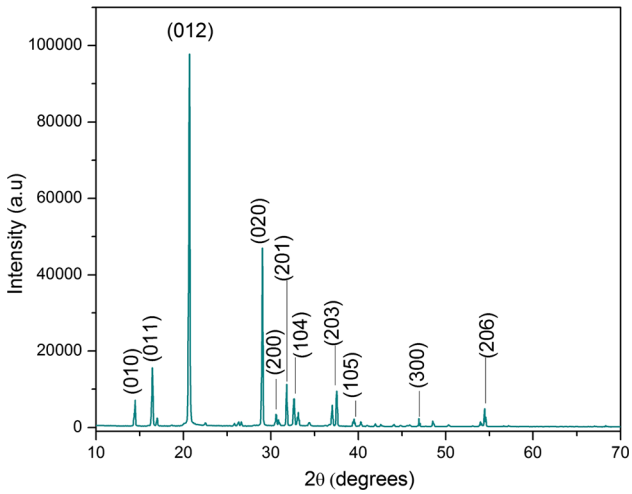

Fig. 2. Powder x-ray diffraction pattern of LACC crystal.

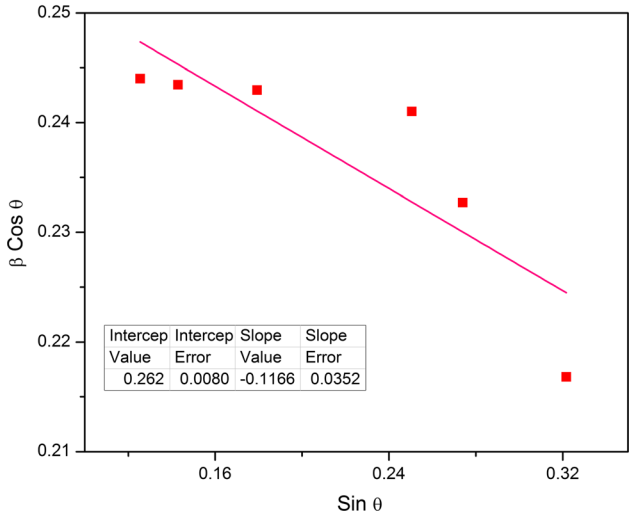

Fig. 3. The plot between $\beta\cos\theta$ versus $\sin\theta$.

was found to be – 0.1166. In general, the negative value of η indicates the vacancy type of defect in the crystals.

FT-IR Analysis

The functional groups of the grown LACC crystal were confirmed using Fourier transform infrared spectroscopy. The molecular vibration of a material and chemical bonding are analyzed using a Perkin-Elmer spectrometer. Figure 4 shows the FTIR spectrum of LACC crystal. The peak observed at 3168 cm^{-1} is due to the asymmetrical stretching vibration of $–NH_3^+$. The asymmetrical bending vibration of NH_3^+ is observed at 2222 cm^{-1} and 2049 cm^{-1}. The peak observed at 1418 cm^{-1} is due to symmetric stretching of CO_2^-. The peak at 1346 cm^{-1} indicates the C-H deformation in CH_3. The sharp peak observed at 1112 cm^{-1} is due to NH_3^+ rocking and C-O Stretching. The presence of CO_2^- (or) C-C-N group deformation vibration is

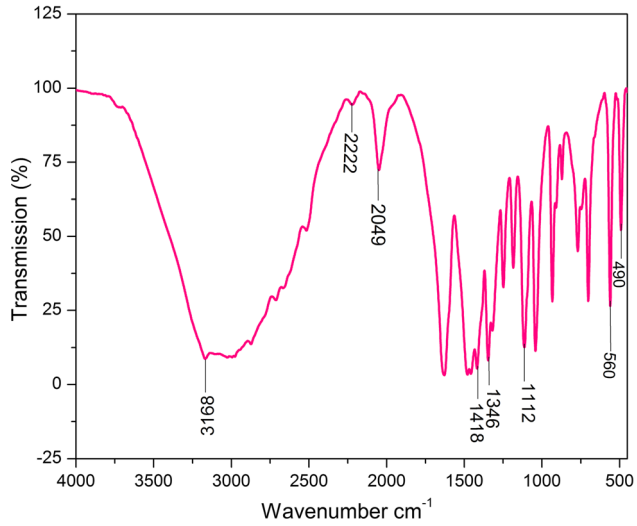

Fig. 4. FTIR spectrum of LACC crystal.

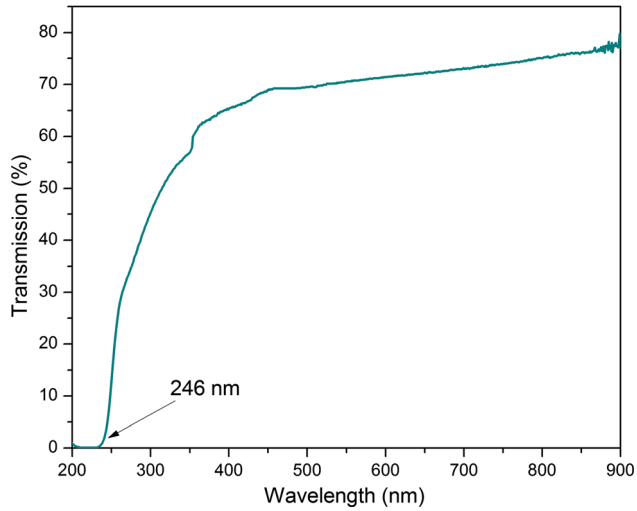

Fig. 5. Optical transmission of LACC crystal.

positioned at 560 cm^{-1}. Torsional vibrations of NH_3^+ are assigned at 490 cm^{-1}. The presence of expected functional groups of LACC crystal was confirmed by FTIR analysis.[12,16]

Optical Studies

The UV–Vis-NIR transmission spectrum of the grown crystal was recorded for the range 200–900 nm and Fig. 5 shows the recorded transmission spectrum. From the transmission spectrum, the LACC crystal exhibits high transmission in the entire visible region nearly 70% with a lower cut-off wavelength at 246 nm. The wide transparency of LACC crystal shows it is more important for optoelectronic device fabrication.[17] The absorption coefficient (α) of the LACC crystal can be calculated using transmission data and it is given by Ref. 18.

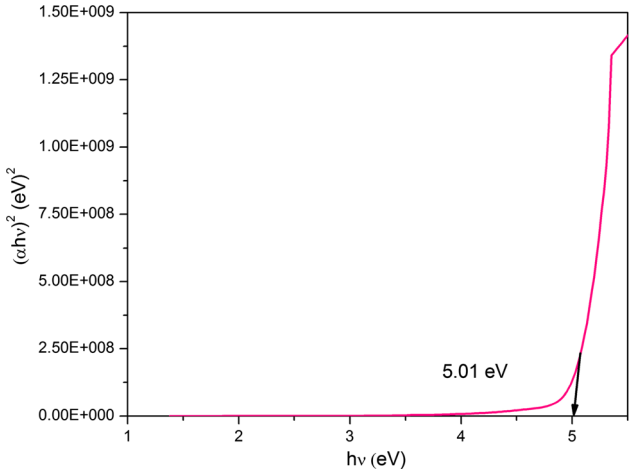

Fig. 6. Tauc's plot of LACC crystal.

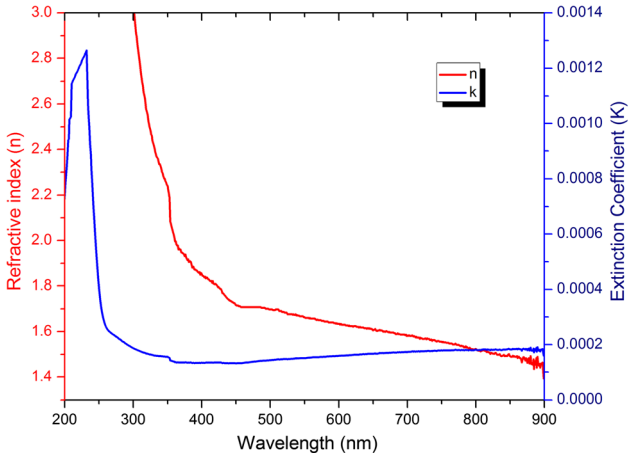

Fig. 7. Variation of the refractive index and extinction coefficient versus wavelength of the LACC crystal.

$$\alpha = \frac{2.303 \log\left(\frac{1}{T}\right)}{t}, \tag{2}$$

where t is the thickness of the crystal, α is absorption coefficient and T is transmission in percentage. The optical transition of LACC crystal is of direct transition nature. The optical band gap was calculated using the relation

$$(\alpha h\nu) = A\left(h\nu - E_g\right)^{1/2}, \tag{3}$$

where α, h, ν, and E_g are absorption coefficient, Plank's constant, frequency and energy gap, respectively. Figure 6 shows the variation of $(\alpha h\nu)^2$ with $h\nu$ in the absorption region.[19] The energy gap of LACC crystal was estimated as 5.01 eV. There by absorption coefficient (α) correlated to the extinction coefficient (K) is shown as,[2]

$$K = \frac{\alpha\lambda}{4\pi} \tag{4}$$

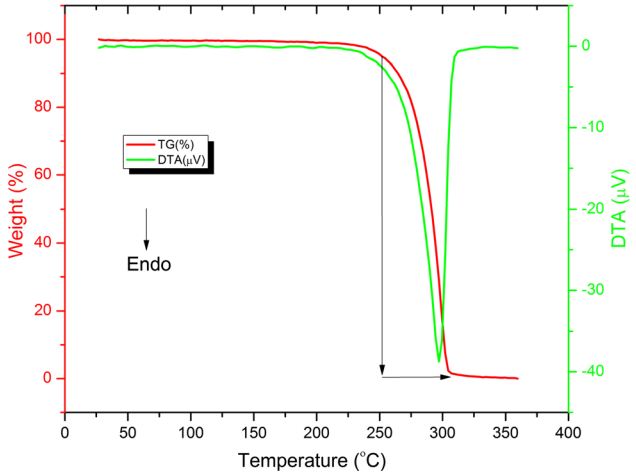

Fig. 8. TG-DTA curve of LACC crystal.

The reflectance (R) in terms of the absorption coefficient can be derived from the following relation.[20]

$$R = \frac{\exp(-\alpha t) - \sqrt{\exp(-\alpha t)T - \exp(-3\alpha t)T + \exp(-2\alpha t)T^2}}{\exp(-\alpha t) + \exp(-2\alpha t)T} \tag{5}$$

The obtained value for the reflectance can be further used to calculate the refractive index of the crystal, using the following relation[21]

$$n = \frac{-\left(R + 1 + 2\sqrt{R}\right)}{(R-1)}. \tag{6}$$

The refractive index of the material was found to be 1.7 in the visible region. Figure 7 shows the variation of the extinction coefficient and refractive index versus wavelength of the LACC crystal.

Thermal Analysis

The thermal stability of the LACC crystal was estimated by thermo-gravimetric (TG) and differential thermal analyses (DTA). The TG-DTA analyses were carried out between 25°C and 370°C at a heating rate of 10 K/min using NETZSCH STA 449 F3 Jupiter analyzer under nitrogen atmosphere and is depicted in Fig. 8. The TG curve shows a single stage decomposition weight loss pattern. The maximum weight loss observed between 233°C and 306°C with a weight loss of 98% is due to the elimination of gaseous molecules. From the TG curve it is observed that the material is found to be thermally stable and suitable for optoelectronics device fabrications. DTA curve shows a single endothermic peak at 298°C which corresponds to melting point of material. A good degree of crystallinity of the crystal is confirmed by the sharp endothermic peak of the DTA curve. Thermal stability of the material is enhanced by doping

Cadmium Chloride, which is an essential condition for device fabrication.

Microhardness Measurement

The microhardness analysis study for the grown LACC crystal was performed by Vicker's diamond pyramidal indenter. The mechanical strength of the material plays an important role in optoelectronic device fabrication. The indentations were made using Vicker's pyramidal indenter for different loads from 10 g to 100 g with a constant indentation period of 10 s for all loads.[22] The hardness of the LACC crystal can be calculated using the relation.[23]

$$H_v = \frac{1.854p}{d^2}\ (\mathrm{kg/mm^2}), \tag{7}$$

where P is the applied load in kg and d is the diagonal length in mm. A plot is depicted in Fig. 9. And shows the variation of Vicker's hardness number with an applied load for LACC crystal. It is clearly seen that LACC crystal has a reverse indentation size effect (RISE) due to the increase of hardness (H_v) as load (P) is increased.[24] The value of the work hardening coefficient is essential to identify the material strength. The Meyer's index (n) value for the soft material is greater than 1.6 and for hard material, it is less than 1.6. The Meyer's index (n) can be determined using the relation.[25]

$$P = Kd^n \tag{8}$$

$$\mathrm{Log}P = \mathrm{Log}K + n\mathrm{Log}d, \tag{9}$$

where K is a constant for a crystal and n is Meyer's index. The Meyer's index (n) is estimated from Fig. 10 which gives variation between log P and log d, by linear fitting. The slope value of the linear fit was identified as n = 3.04, which affirms that the LACC crystal belongs to the soft category. The experimental results ensure that inclusion of dopant in L-alanine increases the mechanical stability which is essential for optoelectronic device fabrications.

Calculation of Nonlinear Parameters

Solid state parameters are important in electro-optic polarizability of the LACC crystal and it is essential for the efficiency of second harmonic generation. The dielectric constant at high frequency depends on the electronic polarizability by valence electron of the material. The plasma energy ($\hbar\omega_p$) is given by Ref. 26.

$$\hbar\omega_p = 28.8\left(\frac{z\rho}{M}\right)^{1/2}, \tag{10}$$

where molecular weight (M) of the crystal is 89.09 g/mol, the sum of valence electron (Z) is 36 and ρ, density of the material is 1.424 g/cm^3. The Penn gap and the Fermi energy of the material were computed using the relations.[27]

$$E_p = \frac{\hbar\omega_p}{\sqrt{(\varepsilon_\infty - 1)}}, \tag{11}$$

$$E_f = 0.2948(\hbar\omega_p)^{4/3}, \tag{12}$$

where ε_r dielectric permittivity of the material at high frequency, E_p is Penn gap and E_f is Fermi energy. Electronic polarizability (α) of the material can be computed using the relation.[28]

$$\alpha = \left[\frac{(\hbar\omega_p)^2 S_0}{(\hbar\omega_p)^2 S_0 + 3E_p^2}\right] \times \frac{M}{\rho} 0.0396 \times 10^{-24}\ \mathrm{cm}^3, \tag{13}$$

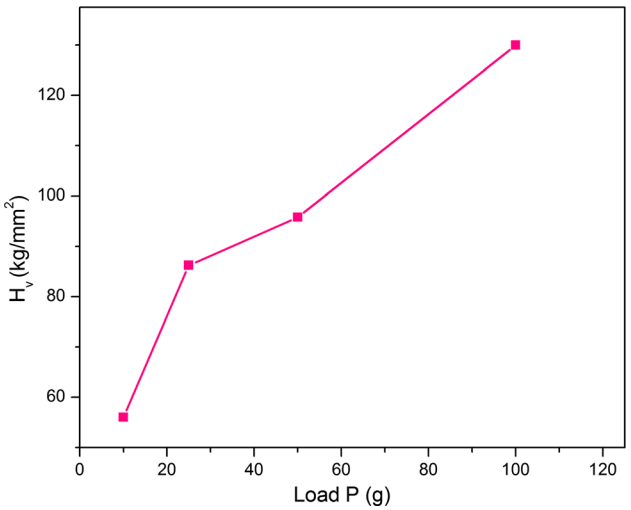

Fig. 9. Variation of Vicker's hardness number and applied load for LACC crystal.

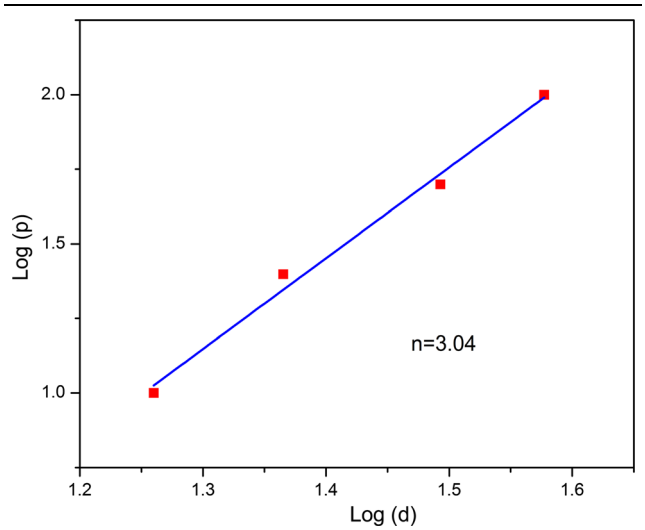

Fig. 10. Variation of log d and log p for LACC crystal.

where S_0 is constant for a particular material which is given by Ref. 29.

$$S_0 = 1 - \left[\frac{E_p}{4E_F}\right] + \frac{1}{3}\left[\frac{E_p}{4E_F}\right]^2 \quad (14)$$

Electronic polaraizability of the grown material was calculated from Eq. 13 and is in good agreement with that from the Clausius–Mossotti relation.[21]

$$\alpha = \frac{3M}{4\pi N_a \rho}\left(\frac{\varepsilon_\infty + 1}{\varepsilon_\infty + 1}\right) \quad (15)$$

The nonlinear parameter values of the grown LACC crystal are shown in Table I.

Kurtz–Perry Powder Second Harmonic Generation Studies

The grown crystals of Cadmium Chloride doped L-alanine crystals were subjected to Kurtz–Perry[30] powder technique for second harmonic generation (SHG) test to confirm the nonlinear optical (NLO) property. The crystals were taken in powder form and tightly packed between glass slides. Nd: YAG Q-switched laser beam of wavelength 1064 nm was made to fall on the powder sample with a pulse width of 6 ns at a repetition rate of 10 Hz. The crystalline samples were powdered and exposed to laser radiation with the input beam energy of 0.701 J. The emission of green light from the sample confirms the second harmonic generation in the crystal. The powder sample of Potassium dihydrogen phosphate (KDP) crystal was used as reference material in the SHG measurement. The output energy of LACC was 13.025 mJ and KDP emitted output energy of 8.94 mJ. The efficiency of LACC crystals was found to be 1.457 times greater than that of the KDP crystals.

Table I. Nonlinear parameter's value of the grown LACC crystals

Parameters	Value
Plasma energy ($\hbar\omega_p$)	21.84 (eV)
Penn gap (E_p)	9.00 (eV)
Fermi energy (E_f)	18.00 (eV)
Electronic polarizability (Penn analysis)	1.56×10^{-23} cm^3
Electronic polarizability (Clausius–Mossoti)	1.64×10^{-23} cm^3
Electronic polarizability (optical band gap)	2.07×10^{-23} cm^3

Laser Damage Threshold Studies

LDT is an essential method for estimating the amount of electromagnetic radiation that can be resisted by an optical component. The LDT value mainly depends on the dislocation density of the material. The material which has less dislocation density can have higher LDT value. The frequency doubling performance of the crystals mainly depends on the surface damage tolerance and the surface damage of the crystal was measured utilizing the following equation.[31]

$$\text{Power density } (P_d) = \frac{E}{\tau A}, \quad (16)$$

where E is the input energy (mJ), τ is a pulse width (6 ns) and A is an area of the spot (mm^2). The calculated LDT value of the LACC crystal was 9.14 GW/cm^2. The calculated LDT value of LACC crystals shows that it has higher value than that of standard NLO material like KDP (0.20 GW/cm^2), urea (1.50 GW/cm^2) and some amino materials such as LHNP (2.04 GW/cm^2)[32] and LAPT (6.72 GW/cm^2).[33] The higher LDT value of LACC shows that it is a suitable candidate for higher power laser application and optoelectronic device fabrication.

Z-Scan Measurement

The nonlinear absorption coefficient (β) and third order nonlinear refractive index (n_2) can be determined by investigating the third order nonlinear properties of LACC crystals using a single beam source of Nd-YAG laser (intensity 50 mW, λ = 532 nm) with beam diameter is 0.5 mm.[20,24] The nonlinear refractive index (n_2) is given by Ref. 34,

$$n_2 = \frac{\Delta\Phi}{KI_0L_{eff}}, \quad (17)$$

where $\Delta\Phi$ is the axial phase shift, I_0 is the intensity of the laser beam at the focus, K is wave vector and L_{eff} is the effective thickness of the material. The nonlinear absorption coefficient (β) is calculated using relation[35]

$$\beta = \frac{2\sqrt{2}\Delta T}{I_0L_{eff}}, \quad (18)$$

where ΔT is the one-Peak value at the open aperture Z-scan curve. The third order nonlinear optical susceptibility ($\chi^{(3)}$) with its imaginary and real parts were computed using the relation,[36]

$$\text{Re}\chi^{(3)} = \frac{10^{-4}\varepsilon_0 c^2 n_0^2 n_2 \Delta\Phi}{\pi}, \quad (19)$$

$$\text{Im}\chi^{(3)} = \frac{10^{-2}\varepsilon_0 c^2 n_0^2 \lambda\beta}{4\pi^2}, \quad (20)$$

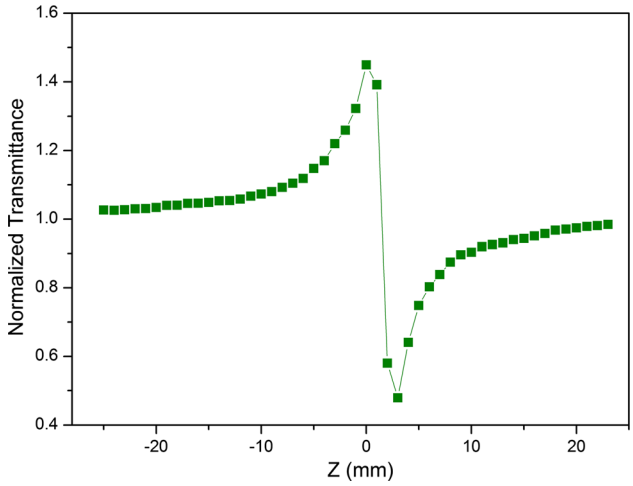

Fig. 11. Closed aperture Z-scan curve of LACC.

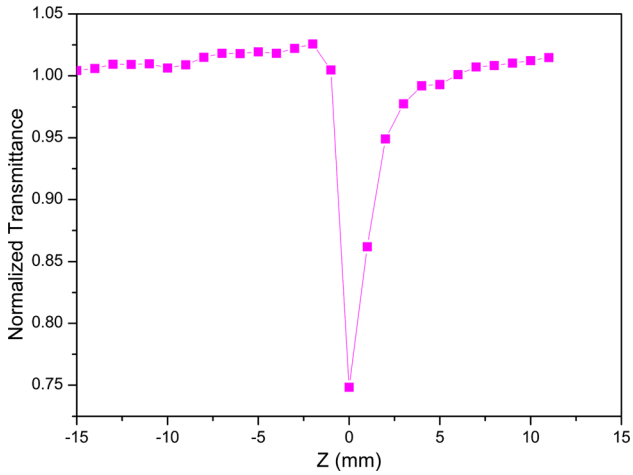

Fig. 12. Open aperture Z-scan curve of LACC.

Table II. Nonlinear optical parameters of the LACC crystals

$n_2 \times 10^{-6}$ (cm^2/W)	$\beta \times 10^{-5}$ (cm/W)	$\chi^{(3)} \times 10^{-5}$ (esu)
3.84	2.41	5.32

where ε_o is the permittivity of the vacuum, c is the velocity of light in vacuum and n_o is the linear refractive index of the sample. The third order nonlinear optical susceptibility of LACC crystal was estimated using the relation,[37]

$$\chi^{(3)} = \sqrt{[\mathrm{Re}(\chi^{(3)})]^2 + [\mathrm{Im}(\chi^{(3)})]^2}. \qquad (21)$$

Z-scan curves of closed aperture and open aperture are shown in Figs. 11 and 12, respectively.

Table III. Comparison of the nonlinear absorption coefficient and third order nonlinear optical susceptibility values of some NLO crystals

β (cm/W)	$\chi^{(3)}$ (esu)	Reference
0.08×10^{-4}	2.74×10^{-6}	$KB_5$35
-5.518×10^{-4}	3.02×10^{-8}	KDNB20
2.41×10^{-5}	5.32×10^{-5}	Present work

From the Z-scan measurements, (β) is the nonlinear absorption coefficient, (n_2) is the nonlinear refractive index and ($\chi^{(3)}$) is third-order nonlinear susceptibility.[37] These parameters were calculated using the above equations and are shown in Table II. The peak followed by a valley in closed aperture shows negative nonlinearity due to self-defocusing. The peak in the open aperture curves shows saturable absorption. The third-order susceptibility of the material was found to be greater than other NLO crystals. The comparison of nonlinearity with some NLO crystals is shown in Table III. Hence, the title material is very much suitable for optoelectronic device fabrication.

CONCLUSION

Optically good transparent cadmium chloride doped L-alanine crystals were grown from aqueous solution by employing the solvent evaporation method. x-ray diffraction studies confirm that the crystal has good crystalline nature, and it belongs to the orthorhombic crystal system. Presence of expected functional groups was confirmed by the FTIR spectrum. From the UV transmission spectrum, energy gap and cut-off wavelength were found to be 5.01 eV and 246 nm, respectively. TG-DTA curve shows the melting point of the crystal to be 298°C. From the hardness study, it is seen that grown LACC crystal belongs to the soft crystal category. Various solid state parameter values of LACC crystals were calculated from measurement. SHG efficiency confirms that the crystal has greater efficiency than KDP. The LDT value of LACC crystals was measured and compared to some standard NLO materials. Z-scan studies show that the material has a large value of the nonlinear optical refractive index (n_2) and nonlinear absorption coefficient (β). The studies carried out on title material conclude that the thermal stability of the material is enhanced due to doping and mechanical strength is increased. Thus, various studies carried out on LACC crystal suggest that the material has great potential for nonlinear optoelectronic device fabrication.

FUNDING

There is no funding involved with the current study.

CONFLICT OF INTEREST

There is no conflict of interest in the work as declared by authors.

REFERENCES

1. A. Alexandar and P. Rameshkumar, *Optik* 168, 944 (2018).
2. P. Sangeetha, P. Jayaprakash, M. Nageshwari, C. Rathika Thaya Kumari, S. Sudha, M. Prakash, G. Vinitha, and M. Lydia Caroline, *Phys. B* 525, 164 (2017).
3. I. Cicili Ignatius, S. Rajathi, K. Kirubavathi, and K. Selvaraju, *Optik* 125, 4265 (2014).
4. T. Thilak, M. Basheer Ahamed, G. Marudhu, and G. Vinitha, *Arab. J. Chem.* 5, 676 (2013).
5. Mohd. Shkir, I.S. Yahia, A.M.A. Al-Qahtani, V. Ganesh, and S. Alfaify, *J. Mol. Struct.* 1131, 43 (2017).
6. S. Arockia Avila and A. Leo Rajesh, *J. Mater. Sci. Mater. Electron.* (2017). https://doi.org/10.1007/s10854-6868-8.
7. R.N. Shaik, Mohd. Anis, M.D. Shirsat, and S.S. Hussaini, *Spectrochim. Acta A* 136, 1243 (2015).
8. S. Masilamani, A. Mohamed Musthafa, and P. Krishnamurthi, *Arab. J. Chem.* 10, S3962 (2017).
9. R.N. Jayaprakash and P. Sundaramoorthi, *Optik* 126, 3570 (2015).
10. Mohd. Shkir, I.S. Yahia, and A.M.A. Al-Qahtani, *Mater. Chem. Phys.* 184, 12 (2016).
11. P.M. Wankhade and G.G. Muley, *Chin. J. Phys.* 55, 2181 (2017).
12. F. Akhtar and J. Podder, *Res. J. Phys.* 6, 31 (2012).
13. I. Cicili Ignatius, S. Rajathi, K. Kirubavathi, and K. Selvaraju, *J. Nonlinear Opt. Phys. Mater.* 25, 1650017 (2016). https://doi.org/10.1142/s021886351650017x.
14. N. Renuka, R. Ramesh Babu, N. Vijayan, G. Bhagavannarayana, and K. Thukral, *Mater. Res. Innov.* 20, 138 (2016).
15. P. Karuppasamy, T. Kamalesh, K. Anitha, S. Abdul Kalam, M. Senthil Pandian, P. Ramasamy, S. Verma, and S. Venugopal Rao, *Opt. Mater.* 84, 475 (2018).
16. G. Socrates, *Book of Infrared characteristic Group* (Hoboken: Wiley, 2001), p. 80.
17. N. Saravanan, S. Santhanakrishnan, S. Suresh, S. Sahaya Jude Dhas, P. Jayaprakash, and V. Chithambaram, *J. Mater. Sci. Mater. Electron.* 29, 18449 (2018).
18. K. Ramachandran, P. Vijayakumar, A. Raja, V. Mohankumar, G. Vinitha, M. Senthil Pandian, and P. Ramasamy, *J. Mater. Sci. Mater. Electron.* 29, 8571 (2018).
19. RO.MU. Jauhar, V. Viswanathan, P. Era, P. Vivek, G. Vinitha, and P. Murugakoothan, *J. Cryst. Growth* 498, 115 (2018).
20. P. Karuppasamy, V. Sivasubramani, M. Senthil Pandian, and P. Ramasamy, *RSC Adv.* 6, 109105 (2016).
21. Sonia, N. Vijayan, M. Vij, P. Kumar, B. Singh, S. Das, Rajnikant, and H. Soumya, *Mater. Chem. Front.* 1, 1107 (2017).
22. P. Rajasekar and K. Thamizharasan, *J. Mater. Sci. Mater. Electron.* 29, 1777 (2018).
23. R. Poornashri Mathangi, A.R. Prabhakaran, S. Nalini Jayanthi, and K. Thamizharasan, *Mater. Today Proc.* 5, 17730 (2018).
24. P. Sangeetha, P. Jayaprakash, M. Nageshwari, M. Peer Mohamed, G. Vinitha, and M. Lydia Caroline, *Chin. J. Phys.* 56, 721 (2017).
25. M. Suresh, S. Asath Bahdur, and S. Athimoolam, *J. Mater. Sci. Mater. Electron.* 27, 4578 (2016).
26. R. Bhuvaneshwari, M. Divya Bharathi, G. Anbalagan, and K. Sakthi Murugesan, *Opt. Mater.* 84, 728 (2018).
27. S. Siva Bala Solanki, N.P. Rajesh, and T. Suthan, *Opt. Laser Technol.* 103, 163 (2018).
28. K. Senthil, S. Kalainathan, Y. Kondo, F. Hamada, and M. Yamada, *Opt. Laser Technol.* 90, 242 (2017).
29. P. Karuppasamy, M. Senthil Pandian, P. Ramasamy, and S. Verma, *Opt. Mater.* 79, 152 (2018).
30. S.K. Kurtz and T.T. Perry, *J. Appl. Phys.* 39, 3798 (1968).
31. S. Kandan, P. Krishanan, R. Jagan, S. Aravindhan, S. Srinivasan, and S. Gunasekaran, *Opt. Mater.* 84, 556 (2018).
32. R.V. Rajan, M. George, J. Alex, D. Sajan, and G. Vinitha, *Opt. Mater.* 86, 198 (2018).
33. V. Thayanithi, K. Rajesh, and P. Praveen Kumar, *Mater. Res. Express* 4, 086201 (2017).
34. A.N. Vigneshwaran, A. Antony Joseph, and C. Ramachandra Raja, *Optik* 127, 5365 (2016).
35. P. Kalaiselvi, S. Alfred Cecil Raj, and N. Vijayan, *Optik* 124, 6978 (2013).
36. P. Karuppasamy, T. Kamalesh, V. Mohankumar, S. Abdul Kalam, M. Senthil Pandian, P. Ramasamy, S. Verma, and S. Venugopal Rao, *J. Mol. Struct.* 1176, 254 (2019).
37. P. Era, RO.MU. Jauhar, G. Vinitha, and P. Murugakoothan, *Opt. Laser Technol.* 101, 127 (2018).